Supplementary information

Design of carbon-ceramic composite membranes with tunable molecular cut-offs from a carboxylic benzoxazine ligand chelated to silica-zirconia

Sulaiman Oladipo Lawal, Hiroki Nagasawa, Toshinori Tsuru, and Masakoto Kanezashi*

Chemical Engineering Program, Graduate School of Advanced Science and Engineering, Hiroshima University, 1-4-1 Kagamiyama, Higashi-Hiroshima 739-8527, Japan

*Corresponding author: E-mail address: kanezashi@hiroshima-u.ac.jp (M. Kanezashi)

SI 1 Materials

The precursor resin sol was prepared via a sol-gel process. Vinyltrimethoxysilane (VTMS; Aldrich; 98 % purity) was used as the silica precursor while zirconium n-butoxide (ZrTB; Aldrich; 80 % in butanol) served as the zirconia precursor. The solvent medium used to carry out the reactions comprised of a 50:50 mixture of dimethyl carbonate (DMC; Nacalai Tesque) and ethanol (EtOH; Aldrich). In the sol-gel reactions, hydrochloric acid (HCl; Nacalai Tesque; 37 % pure) served as the catalyst for hydrolysis. Dibenzoyl peroxide (BzO_2; Aldrich) was used as a radical initiator during thermal curing. All materials were used as received without further purification.

SI 2 Preparation of VTMS-ZrTB-BZPA precursor resin sol, preceramic resin and carbon-ceramic samples

---

The steps involved in the preparation of VTMS-ZrTB-BZPA precursor resin sol up to the preparation of carbon-SiO_2-ZrO_2 are represented in Figure S1. The amounts of the various reagents used are also presented in Table S1.

2 wt% of VTMS-ZrTB-BZPA was prepared in two stages. In the first stage, ZrTB dissolved in DMC was modified by reacting with BZPA (BZPA/ZrTB molar ratio 2:1) for one hour at room temperature. In the second stage, a solution of VTMS in ethanol was then co-hydrolyzed with the BZPA-modified ZrTB (Si/Zr molar ratio 9:1) using deionized water (H_2O/alkoxide molar ratio 4) and HCl as a catalyst (H^+/alkoxide molar ratio 1:4). Hydrolysis and poly-condensation were carried out by stirring the mixture at 600 rpm for more than 12 hours at room temperature.

After the hydrolysis and polycondesation reaction, dibezoyl peroxide (BzO_2) was added (radical initiator/BZPA molar ratio 0.45) to cure the resin sol thermally coupled with slow solvent evaporation in an atmosphere controlled at 80-90 ^oC to obtain the preceramic resin gel. Carbon-SiO_2-ZrO_2 powders were then prepared from VZB preceramic resin gel via pyrolysis at 300 to 850 ^oC under a N_2 stream (600 ml min^{-1}) for 30 minutes.

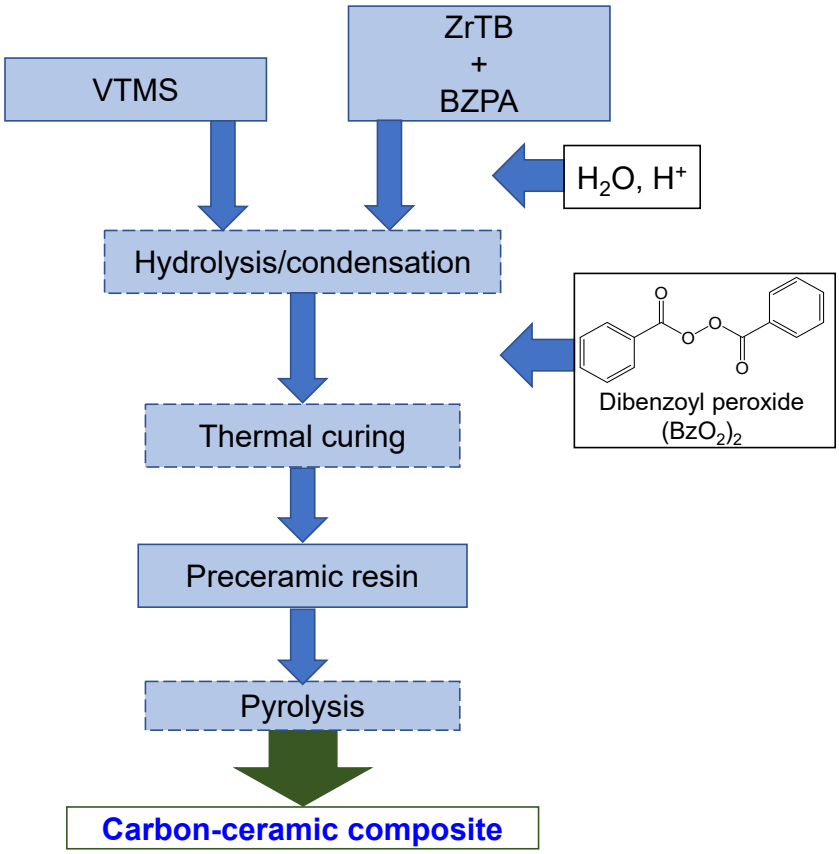

Fig. S1 Preparation flow diagram for VTMS-ZrTB-BZPA resin and derived carbon-ceramic composite

Table S1 Amounts and properties of chemical reagents used in the preparation of VTMS-ZrTB-BZPA resin sol

Reagents	Molar ratios* [-]	Molecular weight [g mol^{-1}]	Purity [%]	Amounts	
				Mole [-]	Mass [g]
ZrTB	0.1	386.7	80	0.00073	0.35
BZPA	0.2	221.2	97	0.00145	0.33
VTMS	0.9	148.2	98	0.00654	0.99
H_2O	4	18	100	0.015	0.26
HCl	0.25	36.5	37	0.0018	0.18

*1 M (molar) basis

SI 3 Characterization of carbon-ceramic samples

The presence and transformation of structural moieties in thin films supported on UV-treated Si-wafers were monitored using Fourier Transform-Infrared spectroscopy (FT-IR, FTIR-4100, JASCO, Japan). The pyrolysis route of the BZPA-modified ZrTB and VZB resin gels were analyzed and monitored using thermogravimetry (DTG-60 Shimadzu Co., Japan). The presence and the chemical states of constituent atoms were confirmed using x-ray photoelectron spectroscopy (XPS; Shimadzu, Japan). The physical evidence of the presence of carbon nanoparticles was confirmed by obtaining the micrographs of the carbon-ceramic particles using transmission electron microscopy (TEM; JEOL, Japan). The samples to be resolved were prepared on ultra-high-resolution carbon supports (STEM 100Cu Grids) by dropping approximately 10 µl of a 2 wt% dispersion of the fine particles in butanol onto the grids. Beforehand, the prepared grids were vacuum-dried at 50 ^{o}C for 24 hours. The crystal/amorphous structure and lattice spacing values of samples were obtained using X-ray diffraction spectroscopy (D2 PHASER X-Ray Diffractometer, Bruker, Germany) with Cu Kα as the radiation source at a wavelength of 1.54 Å. The cross-section morphology and elemental analysis of the carbon-ceramic membrane was examined by Field Emission-Scanning Electron Microscopy (FE-SEM, Hitachi S-4800, Japan). Prior to examination, carefully cut pieces of the membrane were attached to sample holders via carbon tape and vacuum-dried at 50 ^{o}C for 24 hours. Furthermore, N_2 sorption of powders were analysed at -196 ^{o}C using BELMAX sorption equipment (BEL JAPAN INC., Japan). Prior to this measurement, adsorbed gases and vapours were evacuated from the samples at 200 ^{o}C for at least 12 hours.

SI 4 Results and discussion

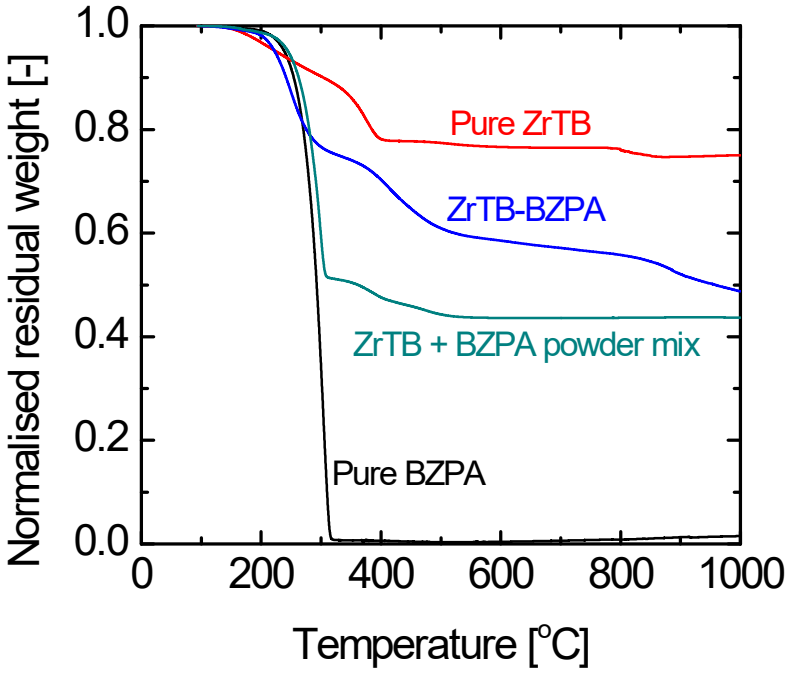

Fig. S2 Thermogravimetry comparison of the decomposition profile of pure BZPA, pure ZrTB, the reaction product of ZrTB and BZPA, and a physically mixed ZrTB and BZPA powders.

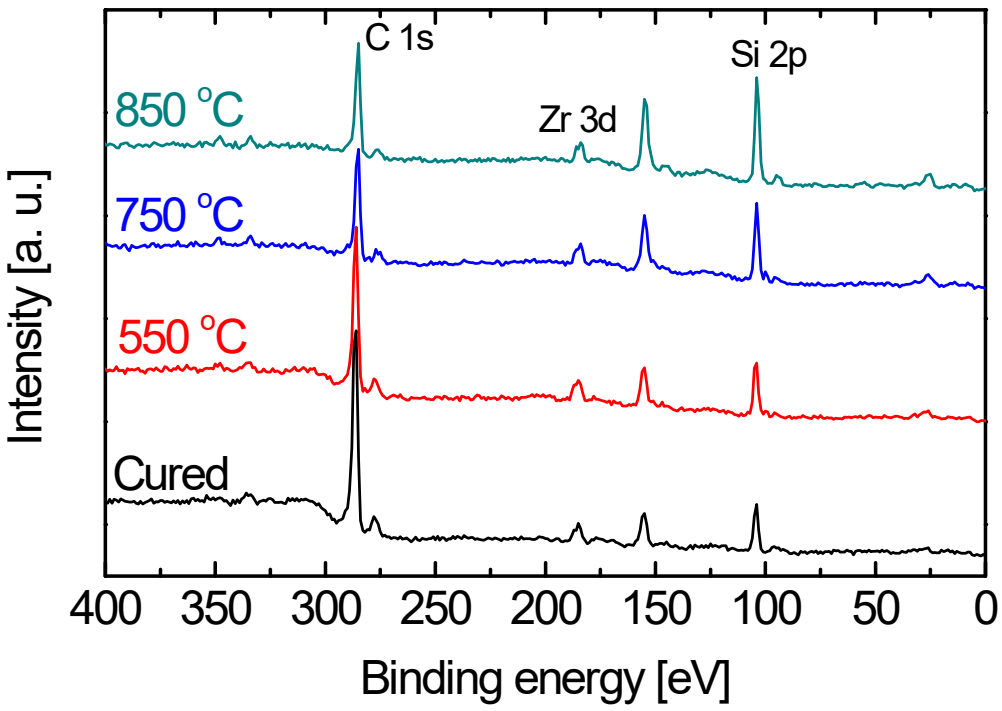

Fig. S3 Survey scan wide x-ray photoelectron spectra (XPS) measured for cured VTMS-ZrTB-BZPA film and derived carbon-ceramic films obtained at different pyrolysis temperatures.

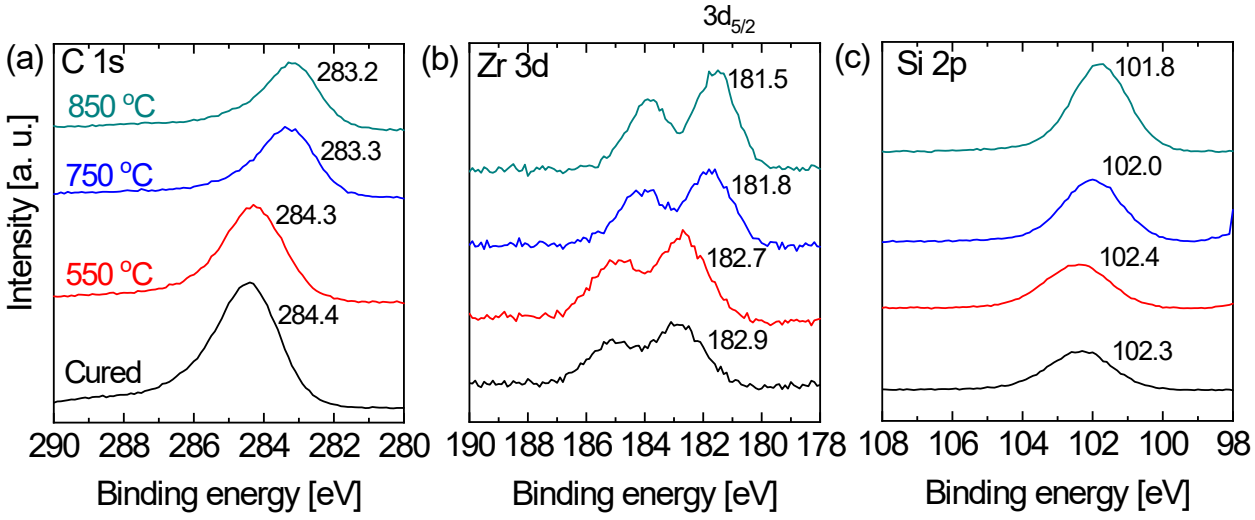

Fig. S4 Narrow (a) C 1s, (b) Si 2p, and (c) Zr 3d XPS spectra of a cured VTMS-ZrTB-BZPA pre-ceramic film and carbon-ceramic films formed at different final pyrolysis temperatures.

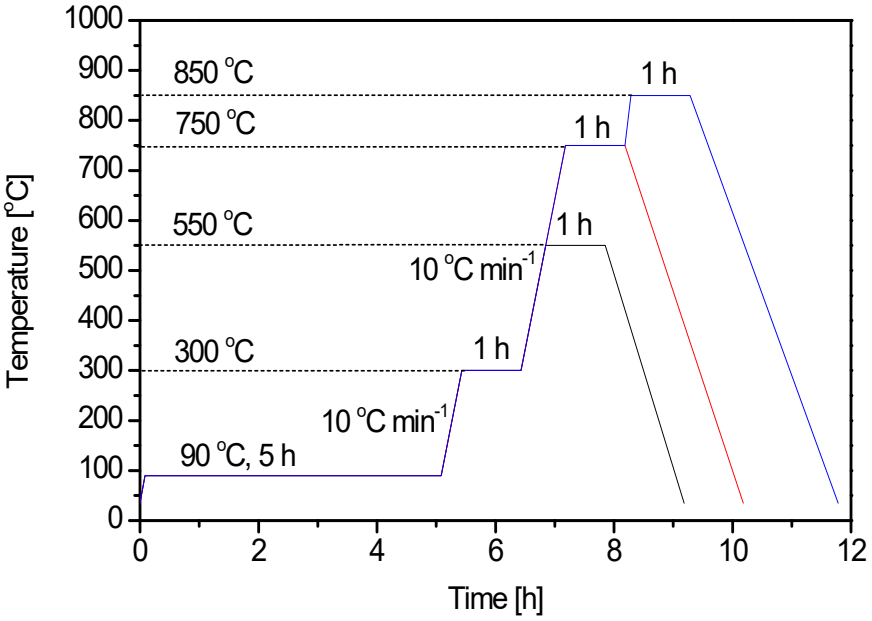

Fig S5. Temperature program used in the fabrication process of C-SZ membranes. The ramping rate between temperatures was 10 °C min^{-1} while the dwell time at each final pyrolysis temperature was 1 hour.

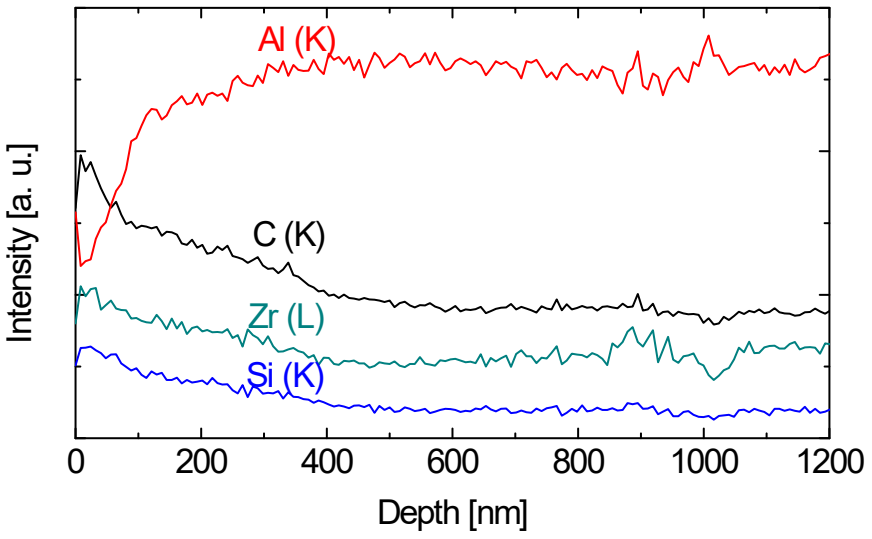

Fig. S6 Atomic EDS intensities of C (K), Al (K), Si (K) and Zr (L) as functions of membrane depth for a carbon-SiO_2-ZrO_2 membrane prepared at 750 °C.

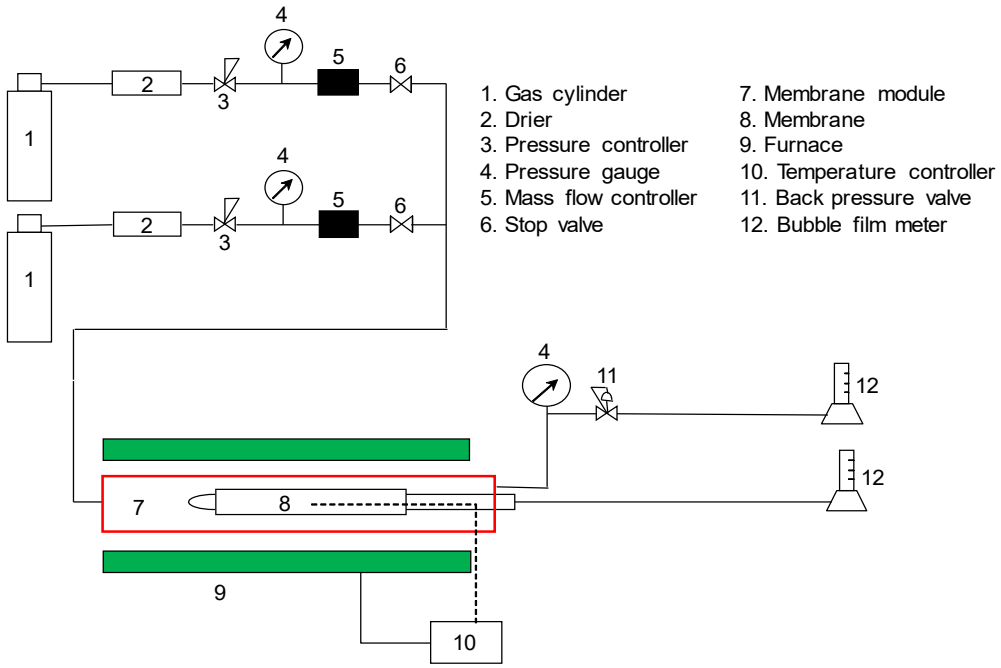

Fig. S7 Flow diagram of the gas permeation rig set-up. The upstream of the membrane module was kept at 200 kPa absolute pressure while the downstream was kept at 100 kPa absolute pressure.

Table S2 H_2 permeance and H_2/CH_4 ideal selectivity for selected state-of-the-art carbon molecular sieve and composite carbon molecular sieve membranes prepared at different pyrolysis temperatures.

Precursor type	Pyrolysis temperature [^oC]	H_2 permeance [10^{-7} mol m^{-2} s^{-1} Pa^{-1}]	H_2/CH_4 ideal selectivity [-]	Reference no.
Carbon molecular sieve membranes				
Polyimide	800	3.13	468	[S1]
Polyimide	700	10.5	228	[S2]
Polyetherimide	600	0.91	174	[S3]
Polyetherimide	900	1.45	100	[S4]
Polyimide	650	0.10	10.5	[S5]
Phenolic resin	850	0.02	45	[S6]
Polyimide	600	1.51	182	[S7]
Phenolic resin	700	0.08	348	[S8]
Cellulose hollow fiber	850	0.5	5706	[S9]
Polyester	500	6.3	250	[S10]
Composite carbon molecular sieve/SiC membranes				
SiC	750	13.7	47	[S11]
SiC	750	15.0	10	[S12]
Phenolic resin/boehmite	600	0.52	1020	[S13]
Phenolic resin/boehmite	600	0.70	1000	[S14]
Fe-doped lignin	500	1.32	584	[S15]
β-SiC	600	0.05	200	[S16]
Carbonized ceramic membranes				
VTMS-Benzoxazine	850	1.94	95	This work

The modified gas translation model proposed by Lee *et al.* [S17] presents a way to estimate the mean pore size of membranes with pore size of less than 1 nm by employing an NKP (normalized Knudsen permeance) method based on the modified gas translation model expressed below.

$$P_i = \frac{1}{3\tau L}\varepsilon(d_p - d_i)\frac{(d_p - d_i)^2}{d_p^2}\sqrt{\frac{8}{\pi M_i RT}}exp\left(-\frac{E_{p,i}}{RT}\right) \quad \text{(S1)}$$

$$P_i = \frac{k_{0,i}}{\sqrt{M_i RT}}exp\left(-\frac{E_{p,i}}{RT}\right) \quad \text{(S2)}$$

Where $\frac{\varepsilon}{3\tau L}\frac{(d_p - d_i)^3}{d_p^2}\sqrt{\frac{8}{\pi}}$ is the pre-exponential factor $k_{0,i}$ expressing the combination of configurational factors of the membrane and permeating molecule (porosity ε, tortuosity τ, membrane thickness L, mean pore diameter d_p and kinetic diameter d_i), $E_{p,i}$ is the apparent activation energy of permeation for a gas species, *i*, M_i is the molecular weight of the gas species, R is the universal gas constant and T is the permeation temperature.

Equation (S2) can be converted as follows.

$$\left(\sqrt{M_i}P_i\right)^{\frac{1}{3}} = \left(\frac{k_0}{\sqrt{RT}}exp\left(-\frac{E_{P,i}}{RT}\right)\right)^{\frac{1}{3}}(d_0 - d_i) \quad \text{(S3)}$$

Where $E_{P,i}$ can be regarded as a constant for the sake of simplicity, and pore size, d_0, can be obtained together with $\frac{k_0}{\sqrt{RT}}exp\left(-\frac{E_{P,i}}{RT}\right)$ by regressing each $\left(\sqrt{M_i}P_i\right)^{\frac{1}{3}}$ to Equation (S3).

To estimate the pore size of the present membranes, $\left(\sqrt{M_i}P_i\right)^{\frac{1}{3}}$ is plotted as a function of the molecular sizes of permeating molecules, d_i, as shown in Figure S8. The molecular size at $\left(\sqrt{M_i}P_i\right)^{\frac{1}{3}} = 0$ corresponds to the pore size, d_0.

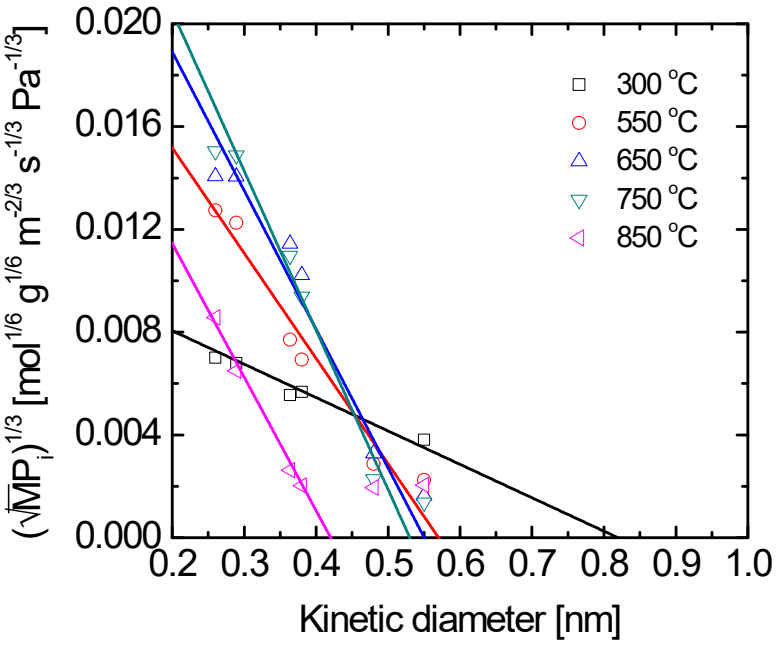

Fig. S8 Linear plot of normalized Knudsen permeance (NKP) as a function of kinetic diameter obtained from the permeation data at 300 °C for the C-SZ membranes

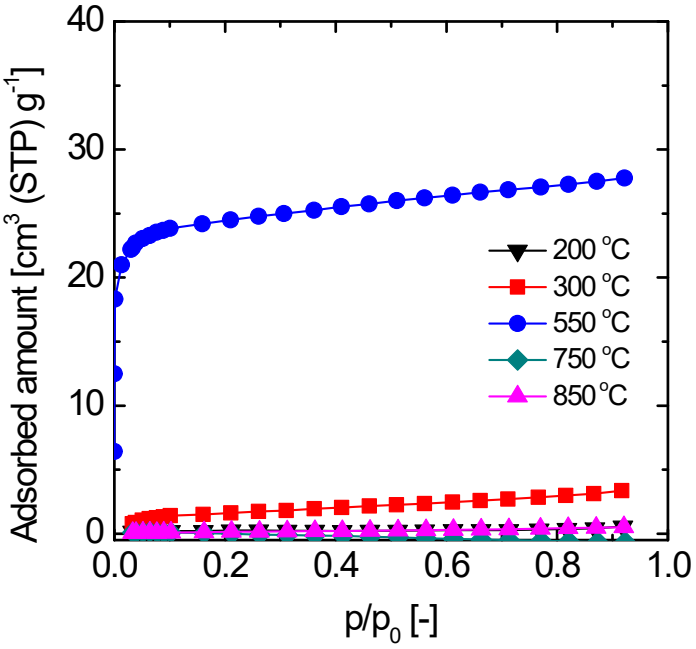

Fig. S9 Nitrogen adsorption isotherms at -196 °C for VZB-derived carbon-SiO_2-ZrO_2 powders obtained at different pyrolysis temperatures.

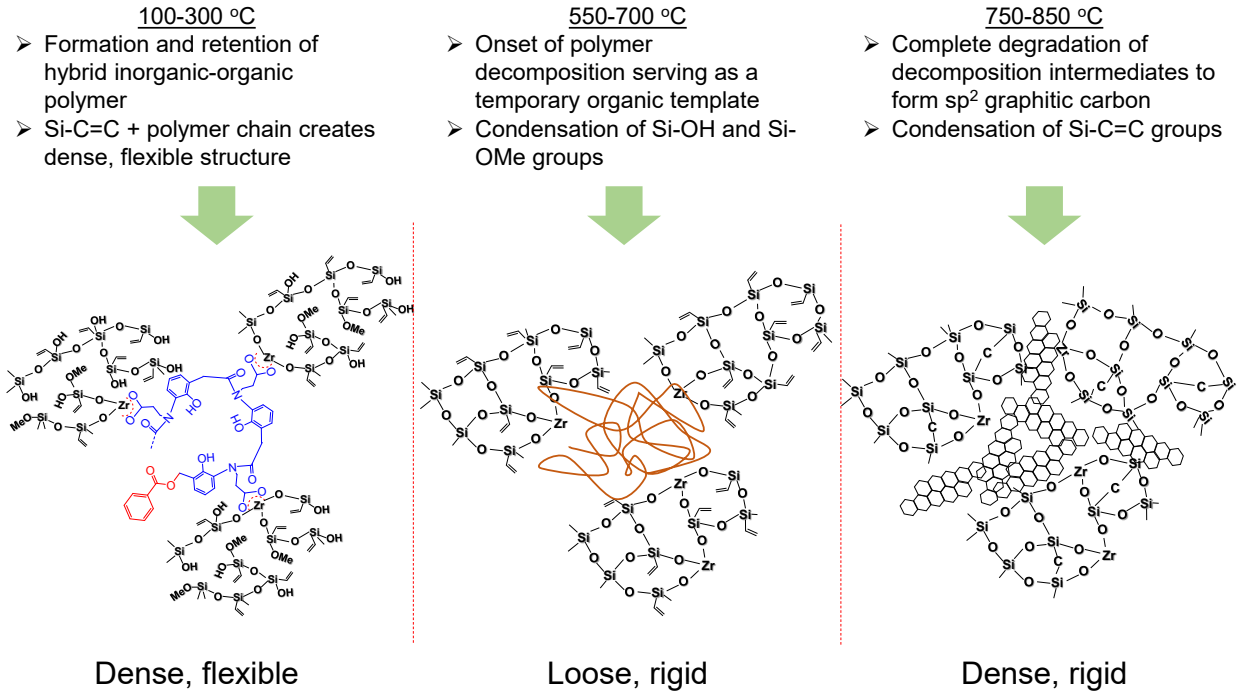

Fig. S10 Schematic illustration of the pyrolytic transformation of a VTMS-ZrTB-BZPA resin into carbon-SiO_2-ZrO_2 structure.

References

S1. W. Ogliego, T. Puspasari, M. K. Hota, N. Wehbe, H. N. Alshareef and I. Pinnau, *Mater. Today Nano*, 2020, **9**, 100065

S2. P. H. Tchoua Ngamou, M. E. Ivanova, O. Guillon and W. A. Meulenberg, *J. Mater. Chem. A*, 2019, **7**, 7082-7091

S3. M. -Y. Wey and H. -H. Tseng, C. -K. Chiang, *J. Membr. Sci.*, 2014, **453**, 603-613

S4. H. -H. Tseng, K. Shih, P. -T. Shiu and M. -Y. Wey, *J. Membr. Sci.*, 2012, **405-406**, 250-260

S5. K. Briceno, D. Montane, R. Garcia-Valls, A. Iulianelli and A. Basile, *J. Membr. Sci.*, 2012, **415-416**, 288-297

S6. W. Wei, G. Qin, H. Hu, L. You and G. Chen, *J. Membr. Sci.*, 2007, **303**, 80-85

S7. M. N. Islam, K. Tanaka, H. Kita and K. -I. Okamoto, *J. Chem. Eng. Jpn.*, 2006, **39(2)**, 131-136

S8. T. A. Centeno and A. B. Fuertes, *J. Membr. Sci.*, 1999, **160**, 201-211

S9. L. Lei, F. Pan, A. Lindbråthen, X. Zhang, M. Hillestad, Y. Nie, L. Bai, X. He and M. D. Guiver, *Nat. Commun.*, 2021, **12:268**, 1-9

S10. H. Richter, H. Voss, N. Kaltenborn, S. Kamnitz, A. Wollbrink, A. Feldhoff, J. Caro, S. Roitsch and I. Voigt, *Angew. Chem. Int. Ed.*, 2017, **56**, 7760-7763

S11. Q. Wang, L. Yu, H. Nagasawa, M. Kanezashi and T. Tsuru, *J Am Ceram Soc.*, 2020, **103**, 4473–4488

S12. Q. Wang, L. Yu, H. Nagasawa, M. Kanezashi and T. Tsuru, *Sep. Purif. Technol.*, **248**, 117067

S13. M. Nordio, J. Melendez, M. van Sint Annaland, D. A. P. Tanaka, M. L. Tanco and F. Gallucci, *Int. J. Hydrogen Energ.*, **45 (53)**, 28876-28892

S14. M. Nordio, J. A. Medrano, M. van Sint Annaland, D. A. P. Tanaka, M. L. Tanco and F. Gallucci, *Energies*, 2020, **13(14)**, 3577

S15. I. Kumakiri, K. Tamura, Y. Sasaki, K. Tanaka and H. Kita, *Ind. Eng. Chem. Res.*, 2018, **57**, 5370−5377

S16. L. -L. Lee and D. -S. Tsai, *J Am Ceram Soc.*, 1999, **82 (10)**, 2796–800

S17. H. R. Lee, M. Kanezashi, Y. Shimomura, T. Yoshioka, and T. Tsuru, *AIChE J.*, 2011, **57**, 2755-2765